Engineering Science and Technology, an International Journal xxx (xxxx) xxx

HOSTED BY

ELSEVIER

Contents lists available at ScienceDirect

Engineering Science and Technology, an International Journal

journal homepage: www.elsevier.com/locate/jestch

Full Length Article

# Modeling and simulation of a high-redundancy direct-driven linear electromechanical actuator for fault-tolerance under various fault conditions

Arun Manohar Gollapudi *, Vasu Velagapudi, Srikanth Korla

*Department of Mechanical Engineering, National Institute of Technology Warangal, Warangal 506004, India*

ARTICLE INFO

*Article history:*
Received 7 September 2019
Revised 21 November 2019
Accepted 30 December 2019
Available online xxxx

*Keywords:*
Fault-Tolerance
High Redundancy Actuator
Electromechanical Actuator
Actuator faults
MATLAB/simscape

ABSTRACT

The high-redundancy actuator (HRA) is a linear displacement actuation system, which consists of a large number of small electromechanical actuation elements arranged in a series and parallel configuration. The performance of a HRA with 9 direct-driven linear electromechanical actuators was analyzed under different fault conditions with the aid of the MATLAB simulation model. The results showed that the HRA has the capability to provide inherent fault-tolerance. Hence, the sudden failure of the system in the presence of fault was avoided. However, the capability of the actuator was found to be reduced gradually depending upon the number of faults.



## 1. Introduction

Faulty elements in any engineering system can be a huge hassle. Sometimes, they might cause irrevocable damage to the industries. Particularly, a fault in the safety-critical system can lead to disasters of unimaginable magnitude. So, designing modern engineering systems with a high level of reliability is of utmost importance to avoid any unexpected failures [1]. One important way this can be prevented is by having a fault-tolerance design that can tolerate any malfunctions of the individual components of the system. In general, fault-tolerance can be achieved by adopting a redundancy technique which includes the addition of resources, time or information beyond the normal requirements of the system being operated.

In recent years, fault-tolerance has become one of the greatest tools for providing safety to any mechatronic system. The aircraft actuation and nuclear power systems are some of the most important systems that need redundancy to ensure reliability [2]. More recently, the aerospace field significantly increased the use of multi redundant electrical actuation systems to avoid unexpected failures [3,4]. However, in the case of nuclear power systems, hardware redundancy is introduced to confirm a high level of reliability of the control system [5].

Traditionally, the fault-tolerance for the actuation system is attained by connecting two or more identical actuators in parallel and the task to be completed by this group of actuators in parallel, is carried out by any one of the individual actuators from the same group. The fact that each of these actuators has the capability to perform the required task alone enables them to override any faulty actuators [6]. However, these actuators in parallel increases the weight and cost of the system and eventually, reduces the efficiency of the system. Moreover, the use of pure parallel configuration holds no value in the event of jamming/lock-up of an actuator within it.

Considering these problems associated with the traditional pure parallel redundancy, the concept of a high-redundancy actuator (HRA) with a grid (both in series and in parallel) configuration was put forward to achieve inherent fault-tolerance. The basic idea behind HRA comes from the behavior of human musculature [7]. The musculature has many individual cells that work in a very typical and ingenious way and the motion provided by each muscle cell contributes very minute to the entire travel and force of the overall muscle system. This is what makes the muscular system highly robust in spite of occasional damage to the individual cells.

By implementing the same concept, the HRA has been designed with many small individual actuation elements that are connected in both series and parallel configuration to form a single actuation

* Corresponding author.
*E-mail address:* arunmanohar.nitw@gmail.com (A.M. Gollapudi).
Peer review under responsibility of Karabuk University.

https://doi.org/10.1016/j.jestch.2019.12.007
2215-0986/

system [8]. The displacement and force provided by each actuation element in the HRA is very small compared to the overall output of the actuation system. The schematic diagram of a HRA with 30 actuation elements is shown in Fig. 1. Here, $X_1$ to $X_5$ are the displacements of the individual actuators and $X_L$ is the overall displacement of the load due to HRA. The base of the actuators that are connected to the fixed support remains immovable while the bases of the other actuators are moveable.

Currently, research on designing HRAs is focused on the use of a small number of electromechanical actuators (EMAs). Previously, a mathematical model for a HRA with 4 electromechanical actuation elements connected in 2 × 2 series-in-parallel configuration under closed-loop conditions was investigated [8]. Results showed that this HRA had the ability to tolerate the faults and in spite of some performance degradation it was able to complete the required task [9]. Another design that was investigated had 16 electromagnetic actuation elements connected in 4 × 4 series-in-parallel configuration under an active fault-tolerance controller and a condition monitoring system that indicates the critical capability level [10,11]. Numerical and experimental work with 12 electromechanical actuation elements connected in 3 × 4 series-in-parallel configuration was also investigated under both open and closed-loop conditions [12].

The present research work aims at developing a 3 × 3 (series and parallel configuration) HRA with 9 direct-driven linear EMAs tested under both healthy and faulty conditions in the simulation environment using MATLAB/Simulink/simscape multibody software tool-box. The main faults considered during the simulation are open and short circuit faults of the motor and jamming and loose faults of the lead-screw. The details regarding the EMA faults are discussed in section 5.1. The main objectives of the present work are:

- Developing a 3D simulation model of a direct-driven linear EMA and a 3 × 3 HRA using MATLAB/simscape multibody.
- Analyzing the performance of this direct-driven linear EMA when connected in pure parallel and pure series configuration under both healthy and faulty conditions in the open-loop.
- Assessing the performance of the HRA model in the open-loop condition under open-circuit, short-circuit, lock-up, and loose faults.

## 2. Linear electromechanical actuator

The electromechanical actuators (EMAs) are a combination of an electric motor (electrical system) and a mechanical gear-box (mechanical system). EMAs are classified into rotary and linear actuators. The linear actuators are further classified into geared and direct-driven linear EMAs. In general, the geared linear electromechanical actuator consists of a DC motor with a lead-screw (or ball-screw or roller-screw) and a nut assembly. The motor shaft is seen connected to the lead-screw with the aid of a shaft-coupling or a gear-box as shown in Fig. 2. The DC motor converts the electrical energy into the rotational motion of the shaft and the lead-screw will then convert this rotary motion into linear motion. The motor shaft will rotate either in the clockwise or anti-clockwise direction depending upon the input polarity. Once the rotations of the shaft are transferred to the lead-screw, the nut makes a translational motion ($X_N$) either in the forward or backward direction depending on the rotational direction of the shaft.

In the direct-driven linear electromechanical actuator, the nut serves as the rotational element and lead-screw acts as the translational element. As shown in Fig. 3, the lead-screw arrangement has been accommodated inside the motor itself. The internally threaded nut is fixed inside the hollow portion of the rotor. When the motor is supplied with electrical energy, both the rotor and the nut rotate and this rotational motion of the nut will help the lead-screw travel linearly. The shaft that is attached to the end of the lead-screw has slotted grooves that restrict the rotational motion of the lead-screw along with the nut. In terms of their function, these two actuators are not very different. However, the direct-driven EMA has a compact size compared to the geared EMA. This is what makes the direct-driven EMA most suitable and appropriate for aerospace industries, robotics, and other industrial machinery.

## 3. A simscape model of a direct-driven linear EMA

Simscape is one of the tool-boxes available for 3D mechanical system simulation in the MATLAB's Simulink library. Using the blocks like bodies, joints, sensor elements that were available in the simscape simulation environment, a 3D model of a direct-driven linear EMA was designed. In the following section, the assembling of individual parts of a single direct-driven EMA modeled in simscape is described in detail.

Initially, the individual bodies of required size and shape (according to Fig. 3) were created using simscape. An assembled direct-driven linear EMA as shown in Fig. 4 was obtained by connecting the individual simscape bodies shown in Fig. 5. The outer hollow casing of the EMA has been sealed on both ends with a bottom and top disc. The bottom disc is nothing but a plane sheet which is fixed at the bottom end of the outer casing with a permanent joint. The two bearings are assembled at the two ends of the rotor with revolute joints between them. This assembled rotor was then placed inside the inner casing which remains to be stationary inside the outer casing. One end of the shaft/lead-screw was inserted into the nut which was inside the rotor and the other end of the shaft with the grooves was extruded out of the top disc.

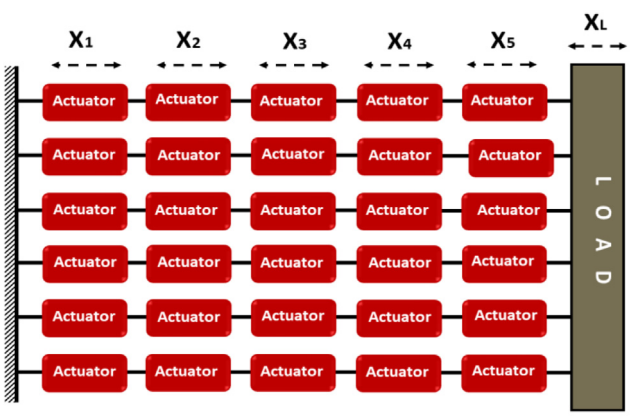


**Fig. 1.** The example of a HRA with 5 × 6 series and parallel configuration.

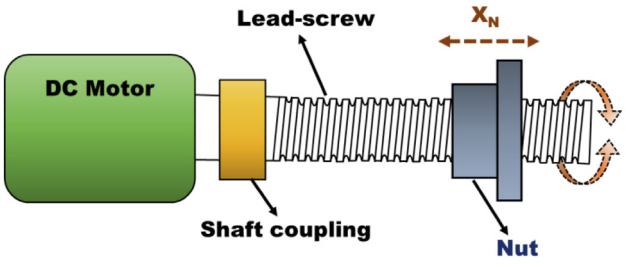


**Fig. 2.** The schematic diagram of a geared linear electromechanical actuator.

Please cite this article as: A. M. Gollapudi, V. Velagapudi and S. Korla, Modeling and simulation of a high-redundancy direct-driven linear electromechanical actuator for fault-tolerance under various fault conditions, Engineering Science and Technology, an International Journal, https://doi.org/10.1016/j.jestch.2019.12.007

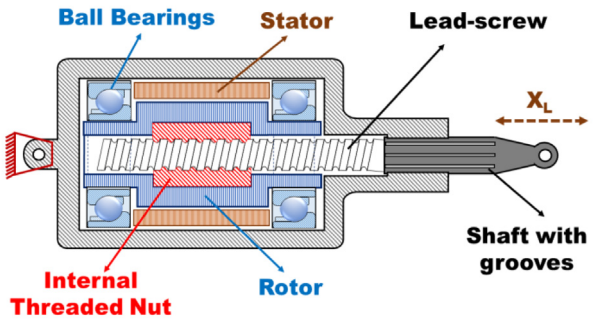


**Fig. 3.** The cross-sectional view of a direct-driven linear EMA.

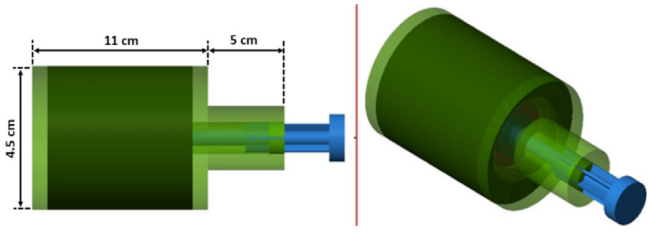


**Fig. 4.** The simscape model of a direct-driven linear EMA.

A lead-screw joint present between the lead-screw and the nut along with the prismatic joint between the shaft and the top disc will ensure the conversion of rotatory motion to translational motion.

For developing the 3 × 3 HRA, Three single EMAs (as shown in Fig. 4) were connected back to back to form a pure series configuration and two more similar series configurations were arranged in parallel. Thus, all the series, as well as the parallel actuation elements will collectively act as a single unit. The simscape model of the HRA developed with 3 × 3 series in the parallel configuration is shown in Fig. 6. The three actuators which are towards the fixed end of the HRA have a fixed base while the other six actuators have a moveable base. The torque which was obtained from the mathematical model of EMA was provided as the input for the simscape EMA model.

## 4. Mathematical modeling of EMA

Modeling of a single EMA is essential for constructing a multi-element actuator like HRA. In this section, the mathematical model of a direct-driven linear EMA is described. Fig. 7 shows the schematic diagram of a motor electrical circuit, lead-screw, dampers and the load of a direct-driven EMA with all the notations indicated.

The electric circuit in the schematic diagram shows that the applied electrical power with a voltage ($V_a$) is opposed by the conducting path resistance ($R_a$), inductance ($L_a$) and a back e.m.f ($V_b$) which is equal to $K_e\left(d\frac{\theta_m}{dt}\right)$. The voltage can then be expressed as:

$$V_a = K_e\left(d\frac{\theta_m}{dt}\right) + R_a i_a + L_a\left(\frac{di_a}{dt}\right) \tag{1}$$

where $K_e$ is the back e.m.f constant and $\theta_m$ is the angular displacement of the motor. In the mechanical system, damping, inertia and frictional properties are concentrated quantities. When the electromagnetic torque generated by the electric circuit is applied to the mechanical system's (lead-screw and nut) rotary element, it rotates at a speed of $d\frac{\theta_m}{dt}$ which has a moment of inertia ($J_m$). The rotational speed of both the rotor and the nut will be the same because they both are attached to each other [13]. $X_s$ and $X_L$ are the linear displacements of the lead-screw and the load respectively. $K_s$ represents the equivalent stiffness that exists between lead-screw and nut and the damping that exists between bearing and rotor is

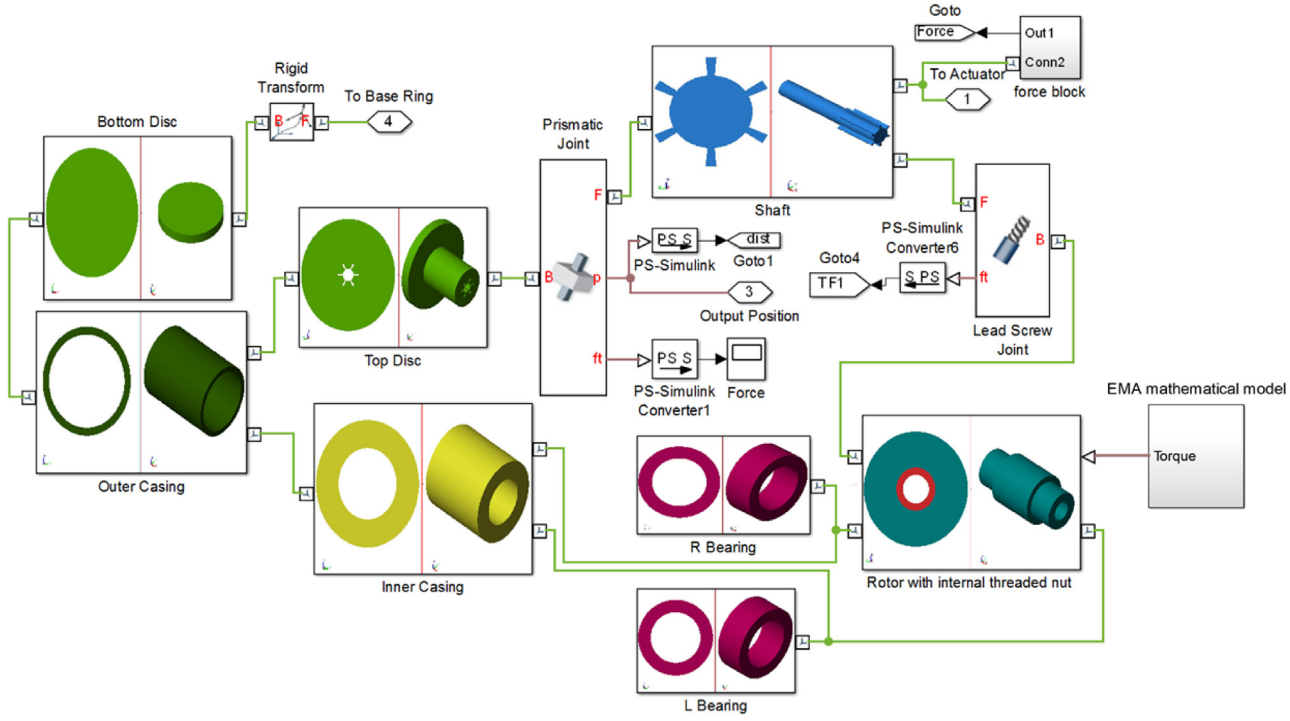


**Fig. 5.** The block diagram showing the arrangement of direct-driven linear electromechanical actuator bodies in simscape module.

Please cite this article as: A. M. Gollapudi, V. Velagapudi and S. Korla, Modeling and simulation of a high-redundancy direct-driven linear electromechanical actuator for fault-tolerance under various fault conditions, Engineering Science and Technology, an International Journal, https://doi.org/10.1016/j.jestch.2019.12.007

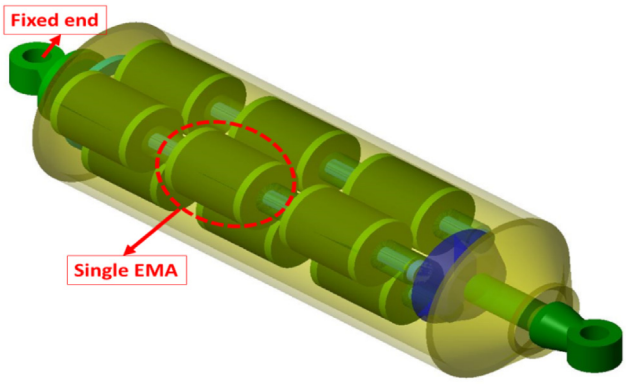


**Fig. 6.** The simscape model of a 3 × 3 HRA with direct-driven linear EMA.

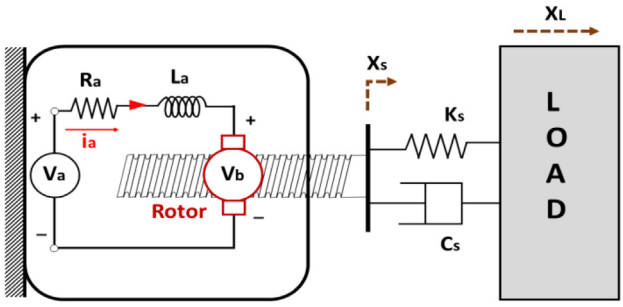


**Fig. 7.** The schematic diagram of a direct-driven linear EMA.

represented by $C_s$. The generated torque $(\tau_m)$ is opposed by damping torque $(\tau_d)$, load torque $(\tau_l)$ and an inertial torque $(\tau_i)$. Hence, the generated electromagnetic torque is balanced by the other three torques as expressed in Eq. (2).

$$\tau_m = \tau_d + \tau_l + \tau_i \tag{2}$$

$$\tau_m = K_t i_a \tag{3}$$

$$\tau_d = D\left(\frac{d\theta_m}{dt}\right) \tag{4}$$

where D is the equivalent viscous damping coefficient at the armature

$$\tau_i = J_m\left(\frac{d^2\theta_m}{dt^2}\right) \tag{5}$$

$$\tau_l = \left(\frac{C_s l}{2\pi}\right)\left(\dot{X}_s - \dot{X}_L\right) + \left(\frac{K_s l}{2\pi}\right)(X_s - X_L) \tag{6}$$

The torque $(\tau_m)$ generated by the current $(i_a)$ which is passing through the armature is given by the Eq. (3). $K_t$ represents the motor torque constant. Similarly, the damping, inertial and load torques are given in the subsequent Eqs. (4)–(6) respectively. In Eq. (6), the term $\left(\frac{l}{2\pi}\right)$ is used for converting the angular displacement of the nut to linear displacement of the lead-screw, where $l$ is the screw lead.

The parameters shown in Table 1 were used as input for solving the equations using MATLAB/Simulink. The torque output obtained from the mathematical model was then provided as the input for each EMA modeled in the simscape. The mathematical model solved in MATLAB/Simulink is shown in Fig. 8. The input voltage provided is a square pulse varying from 6 V to −6 V which makes the motor rotate in the clockwise and anti-clockwise direction. So, the linear actuator will make forward and backward movements accordingly.

**Table 1**
Parameter values.

| S.No | Parameter notation | Value |
|---|---|---|
| 1 | $V_a$ | 6 V |
| 2 | $R_a$ | 0.4 Ω |
| 3 | $L_a$ | 0.8 mH |
| 4 | D | $8.2985e^{-4}$ Nm/rads$^{-1}$ |
| 5 | J | $4.4574e^{-5}$ kgm$^2$ |
| 6 | $K_e$ | 0.036867 V/rads$^{-1}$ |
| 7 | $K_t$ | 0.030892 Nm/A |
| 8 | l | 0.002 m/rev |
| 9 | $C_s$ | 25610 N/ms$^{-1}$ |
| 10 | $K_s$ | 201060000 N/m |

## 5. Fault, failure and graceful degradation

Any fault in the system will deviate that system from its normal performance or behavior. Fault can be expressed as the occurrence of an unpredictable defect in the software or hardware of the system. On the other hand, failure is expressed as a permanent interruption to the ability of the system to carry out a required function. According to [14], the term fault is used to represent a malfunction of the system rather than a disaster, while the term failure is used to represent a complete breakdown.

The concept of fault, graceful degradation and failure can be represented by a simple diagram as shown in Fig. 9. The performance value of the system that is operational can lie within the acceptable or graceful degradation or unacceptable regions and this is determined by the degree of fault. The innermost point (Pn, shown in green) represents a system without any faults, showing nominal performance. As evident from the diagram when the degree of fault is minimum, the deviation of the system will also be minimum and the performance of the system will remain in the acceptable region (represented in white). Under these circumstances, the system withstands these faults and achieves complete fault tolerance. A system that attains complete fault-tolerance will fall under the acceptable region. If the system is able to perform without a complete breakdown in spite of an increased degree of faults, then the system is said to be within the graceful degradation region. So, the system that attains the partial fault-tolerance will lie within the graceful degradation region. When the performance values of the system deviate beyond the graceful degradation value then the system will collapse and is considered to be in the unacceptable region.

### 5.1. Common faults in EMA

As EMA is a combination of electrical and mechanical elements, there is an equal chance of occurrence of a fault in either of these elements. Although there are many faults that can occur in both the elements [15], Researchers mainly focused on the common faults which cause the individual actuators to fail. The most common mechanical faults considered are lock-up fault and the loose fault. Similarly, most common electrical motor faults that are considered include open-circuit (OC) and short-circuit (SC) faults.

OC fault in the motor can occur due to the breakage of one or more turns in the winding phase. When this happens, the flow of current becomes zero in the fault phase and there is no torque generation by the motor. This fault can be simulated in the simulation model by keeping the current passing through the winding and the torque of the motor as zero for a particular actuator. SC fault occurs when turns inside the windings are shorted together. Depending

Please cite this article as: A. M. Gollapudi, V. Velagapudi and S. Korla, Modeling and simulation of a high-redundancy direct-driven linear electromechanical actuator for fault-tolerance under various fault conditions, Engineering Science and Technology, an International Journal, https://doi.org/10.1016/j.jestch.2019.12.007

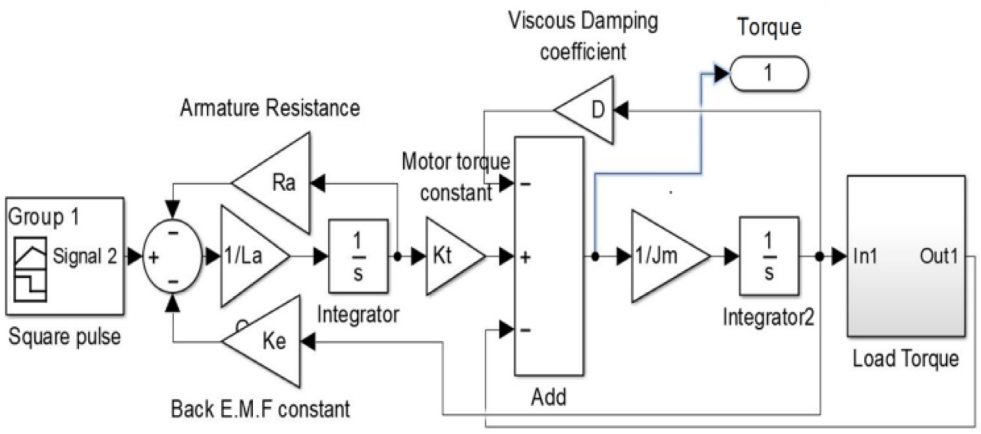


**Fig. 8.** Simulink block diagram of a single EMA mathematical model.

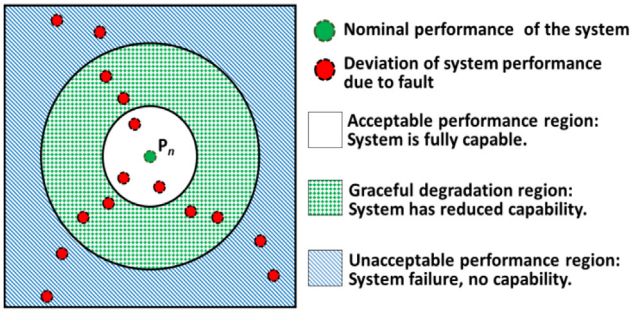


**Fig. 9.** Concept of fault, failure and graceful degradation.

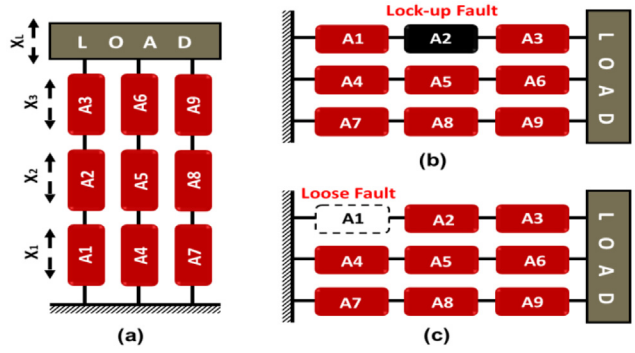


**Fig. 10.** Block diagram of a 3 × 3 HRA (a) Healthy condition (b) with A2 actuator lock-up fault (c) with A1 actuator loose fault.

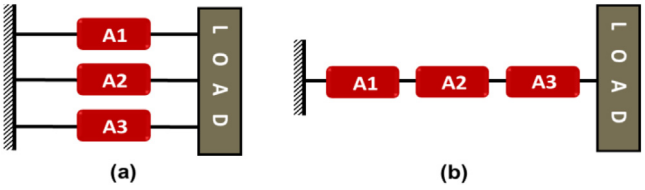


**Fig. 11.** (a) A pure parallel configuration (b) A pure series configuration.

on the number of short turns, a significant change in the resistance, mutual and self-inductance and also the back e.m.f changes occur. However, no positive torque is generated. This fault can be simulated by setting the supply voltage of a particular actuator to zero.

Lock-up or jamming fault occurs when lead-screw or ball-screw nut gets jammed. This happens because of fragmentation or deformation of the balls or because of the locking of the gears in the gear-box. This results in the failure of the transmission of the actuator. To analyze the consequences of this fault in the HRA, the fault was introduced into the simulation model manually by making the displacement of a particular actuator as zero. Loose fault results from loss in applied force between the mechanical elements or the free movement of the lead-screw without any restriction/force. This fault can be modeled by making the output force of the element, zero, which is equivalent to making the input voltage, zero. Hence, there is not much variation in the effect due to SC fault and loose fault. For this particular simulation, both faults under consideration were treated as equal.

The 3 × 3 HRA actuation elements numbering and the representation of lock-up and loose faults are shown in Fig. 10. The actuator under the lock-up fault will act as a rigid element and the actuator under the loose fault will act like there is no physical connection between the ends. Figs. 11a and b shows the pure parallel and pure series configuration with 3 actuation elements.

## 6. Results and discussion

In the initial stage, the performance of 3 actuators connected in a pure parallel configuration and 3 actuators connected in the pure series configuration were analyzed under both healthy and faulty conditions. When the actuators were moving in the forward and backward direction, the linear displacement, force and the linear velocities of the actuators with respect to time were plotted. Figs. 12a and 12b shows the performance of actuators connected in pure parallel and in a pure series configuration.

In the pure parallel configuration, there is no variation in the linear displacement and velocity of the actuator compared to the single actuator's linear displacement and velocity which is equal to 2.323 cm and 12.04 cm/s respectively. However, the force increased by three times (from 26.8 N to 80.39 N) that of a single actuator's force. In the Pure series configuration, the linear displacement and linear velocities increased by three times i.e. 2.346 cm to 7.027 cm and 12.03 cm/s to 36.09 cm/s respectively. The forces of all the 3 actuators in the series is expected to be the same. However, the first/single (A1) actuator experiences more impact due to the mass of the second (A2) and third (A3) actuators. Similarly, the actuator A2 also experiences some impact due to the mass of the third (A3) actuator. Because of this reason, the force exerted by the first/single (193.9 N) actuator is more than the

Please cite this article as: A. M. Gollapudi, V. Velagapudi and S. Korla, Modeling and simulation of a high-redundancy direct-driven linear electromechanical actuator for fault-tolerance under various fault conditions, Engineering Science and Technology, an International Journal, https://doi.org/10.1016/j.jestch.2019.12.007

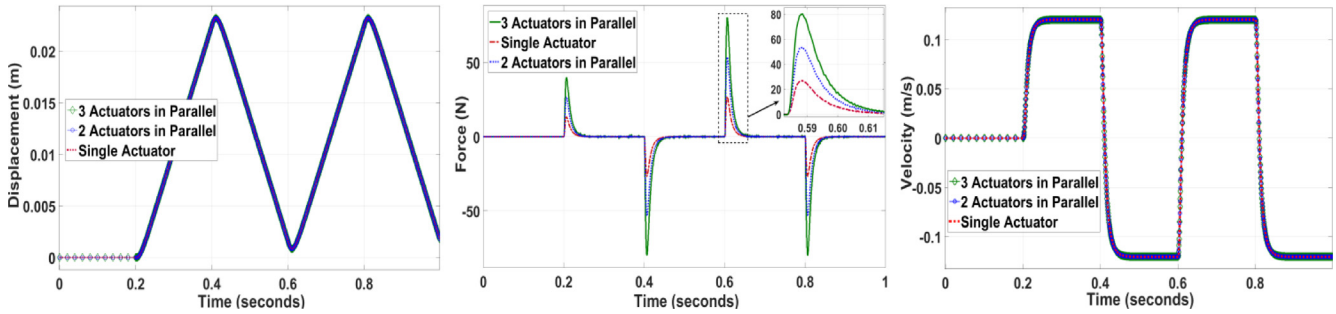


**Fig. 12a.** The displacement, force, and velocities of first, second and third actuators which are connected in a pure parallel configuration.

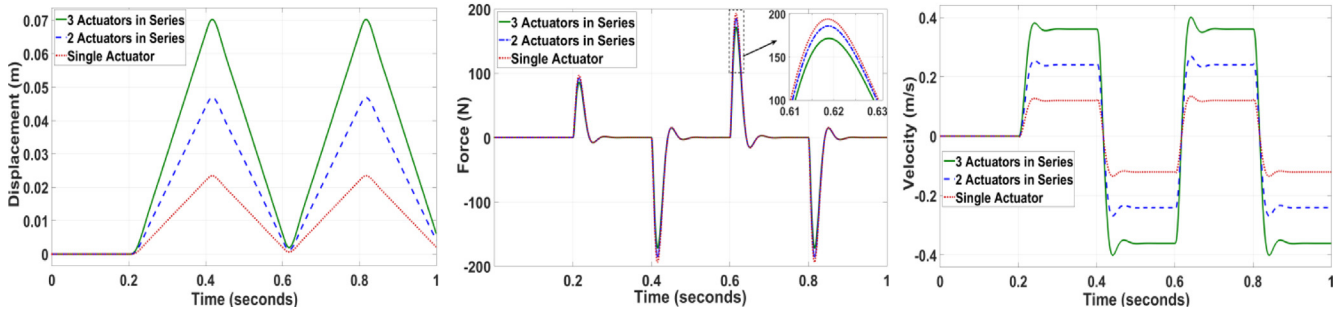


**Fig. 12b.** The displacement, force, and velocities of first, second and third actuators which are connected in a pure series configuration.

overall force (171.6 N) of the series actuators as shown in the force plot in Fig. 12(b). The values showing the performance of the pure parallel and pure series configurations without introducing faults are provided in Table 2.

The Figs. 13(a) and 13(b) are the plots obtained by introducing the lock-up, loose/SC and OC faults in pure parallel and in a pure series configuration with 3 actuation elements. The pure parallel configuration was unable to overcome loose/SC fault. As evident from the plot, the displacement value reduced from 2.323 cm to 1.548 cm and the force reduced from 80.39 N to 53.33 N. In case there is a lock-up fault in any of the actuators connected in the parallel configuration, the displacement becomes zero because the locked-up element acts as a rigid link. However, the other two actuation elements which are in parallel will continue to exert the force on the load. Because of this reason, the force increased drastically (80.39 N to 970.4 N) as evident from Fig. 13(a). In such a situation, the entire system fails. Similarly, in the presence of OC fault, the displacement of the actuator was completely distorted but the force exerted showed only minor variation (52.58 N). All the values showing the performance of the pure parallel and pure series configurations with the introduced faults are provided in Table 3. The pure series configuration was able to tolerate all types of faults and showed a graceful degradation with each of them. However, the force under loose/SC fault is a bit less (108 N) compared to other force values.

The performance of a 3 × 3 HRA was analyzed by introducing lock-up, SC/loose and OC faults independently. The faults were introduced one by one into the HRA starting from A1 to A9 and following the sequence of A1, A4, A7, A2, A5, A8, A3, A6 and A9 (refer Fig. 10). To avoid the confusion by plotting all the 9 faulty actuation element results in a single plot it was divided into 3 results per plot. Figs. 14(a), 14(b) and 14(c) show the resultant linear displacement, force and linear velocity of the 3 × 3 HRA under lock-up fault respectively. The results show that the HRA can tolerate up to 6 lock-up faults by degrading the performance from 7.007 cm to 2.323 cm of displacement and force from 204.4 N to 79.96 N. However, it fails immediately if the faults are increased beyond 6. Table 4 gives the values of displacement, force, and velocity of 3 × 3 HRA under lock-up faults.

The performance values of the HRA under SC/loose faults are provided in Table 5 and the resultant displacement, force, and velocity are shown in Figs. 15(a), 15(b) and 15(c) respectively. The HRA under the SC/loose fault can operate up to a failure of 8 actuation elements with a graceful degradation from 7.007 cm to 0.8 cm of displacement and 204.4 N to 21.6 N of force. However, the force exerted by the actuator under the SC/loose fault was the minimum value compared to the force exerted due to other fault types. The Figs. 16(a), 16(b) and 16(c) show the linear displacement, force and linear velocities of the 3 × 3 HRA under OC fault. The HRA can tolerate up to 6 OC faults with a graceful degradation of displacement from 7.007 cm to 2.33 cm and force from 204.4 N to 64.66 N. Introducing faults further will make the system to behave unusually. The values of all the OC faults are given in Table 6.

**Table 2**
Performance of Pure Parallel and Pure Series configuration of 3 actuators without fault.

| S.No. | Output | Actuators in Parallel | | | Actuators in Series | | |
|---|---|---|---|---|---|---|---|
| | | Fixed/1st actuator | Middle/2nd actuator | Last/3rd actuator | Fixed/1st actuator | Middle/2nd actuator | Last/3rd actuator |
| 1 | Displacement (cm) | 2.323 | 2.323 | 2.323 | 2.346 | 4.687 | 7.027 |
| 2 | Force (N) | 26.8 | 53.59 | 80.39 | 193.9 | 185.7 | 171.6 |
| 3 | Velocity (cm/s) | 12.04 | 12.04 | 12.04 | 12.03 | 24.04 | 36.09 |

Please cite this article as: A. M. Gollapudi, V. Velagapudi and S. Korla, Modeling and simulation of a high-redundancy direct-driven linear electromechanical actuator for fault-tolerance under various fault conditions, Engineering Science and Technology, an International Journal, https://doi.org/10.1016/j.jestch.2019.12.007

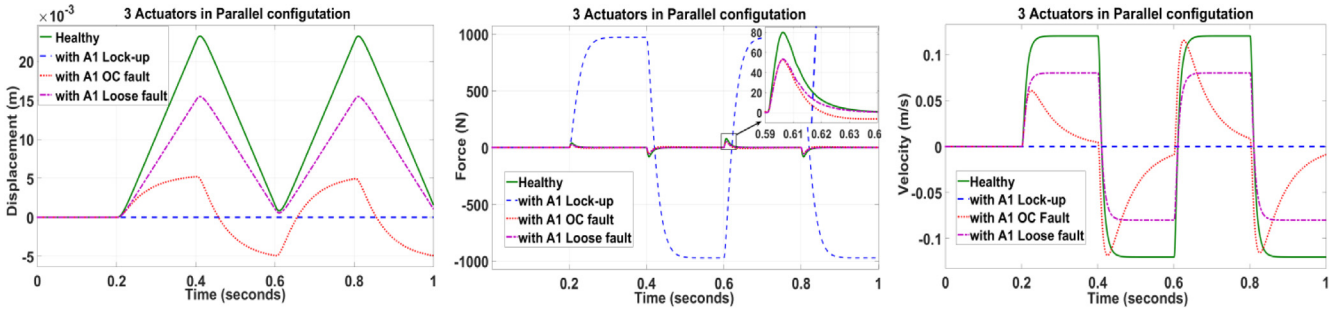


**Fig. 13a.** The comparison of displacement, force, and velocities of a pure parallel configuration with 3 actuators, when actuator A1 subjected to lock-up, open-circuit and short-circuit/loose faults individually.

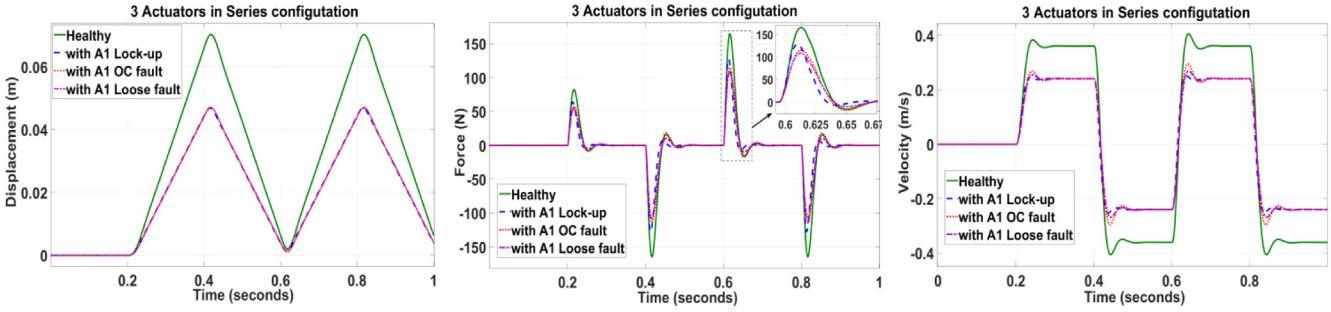


**Fig. 13b.** The comparison of displacement, force, and velocities of pure series configuration with 3 actuators, when actuator A1 subjected to lock-up, open-circuit and short-circuit/loose faults individually.

**Table 3**
Performance of the Pure Parallel and Pure Series configuration of 3 actuators with faults.

| S.No. | Fault | Actuators in Parallel | | | Actuators in Series | | |
|---|---|---|---|---|---|---|---|
| | | Displacement (cm) | Force (N) | Velocity (cm/s) | Displacement (cm) | Force (N) | Velocity (cm/s) |
| 1 | Healthy | 2.323 | 80.39 | 12.04 | 7.027 | 164.6 | 36.17 |
| 2 | Lock-up | 0 | 970.4 | 0 | 4.679 | 127.3 | 24.07 |
| 3 | Open circuit | 0.52 | 52.58 | 6.06 | 4.712 | 114.5 | 24.0 |
| 4 | Loose/short-circuit | 1.548 | 53.33 | 8.022 | 4.678 | 108.0 | 24.05 |

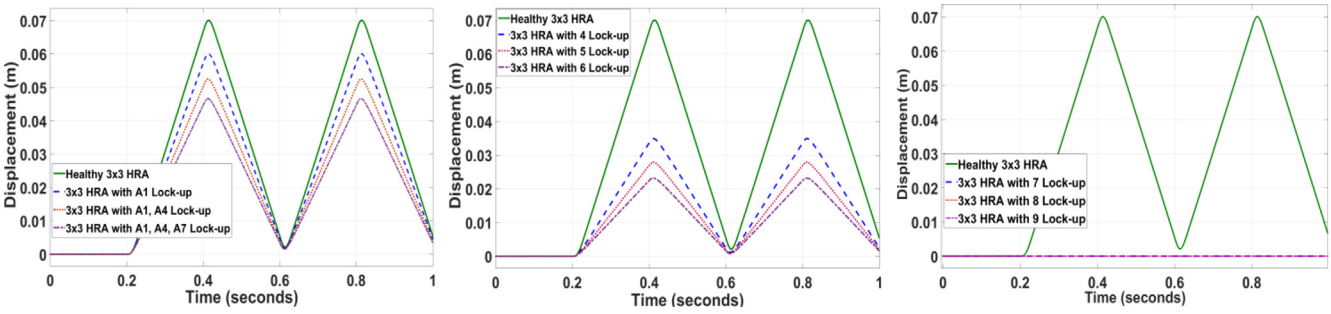


**Fig. 14a.** Displacements of 3 × 3 HRA under increasing the number of lock-up faults in the actuator from A1 to A9 (column-wise).

## 7. Conclusion

The High-Redundancy Actuator (HRA) we designed proved to have many advantages compared to the pure parallel configurations that are in existence. Some of the advantages include; improved reliability, size reduction, reduced weight, and reduced cost of the actuation system. As a part of the current work, we mainly focused on the behavior of the 3 × 3 HRA under a number of fault conditions in the simulation environment as discussed above. Our results showed an increase in the number of faulty elements in a HRA will reduce the performance of actuation gradually. However, the chances of sudden failure of the system are unlikely.

The pure series configuration of 3 actuation elements that we studied showed that the travel capability improved by three times (i.e. from 2.323 cm to 7.027 cm) and the velocity also enhanced by three times (i.e. from 12.03 cm/s to 36.09 cm/s). The results also showed that a system with 3 actuators in a series configuration can tolerate the lock-up fault, open-circuit fault, and short-circuit/loose fault. As long as the failure is limited to 2 actuation

Please cite this article as: A. M. Gollapudi, V. Velagapudi and S. Korla, Modeling and simulation of a high-redundancy direct-driven linear electromechanical actuator for fault-tolerance under various fault conditions, Engineering Science and Technology, an International Journal, https://doi.org/10.1016/j.jestch.2019.12.007

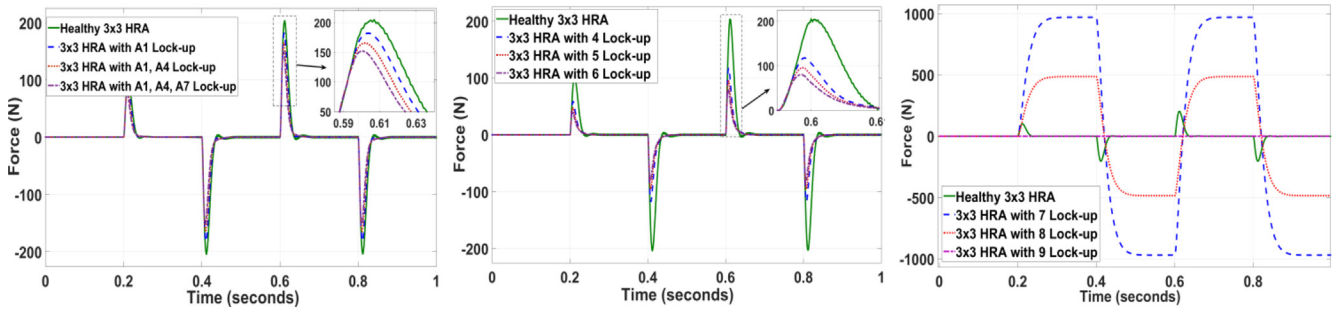


**Fig. 14b.** Force induced due to 3 × 3 HRA under increasing the number of lock-up faults in the actuator from A1 to A9 (column-wise).

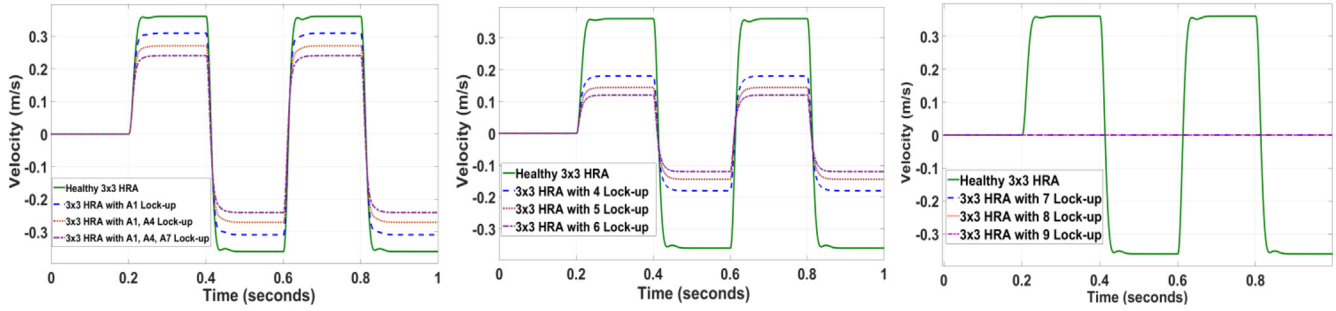


**Fig. 14c.** Velocities to 3 × 3 HRA under increasing the number of lock-up faults in the actuator from A1 to A9 (column-wise).

**Table 4**
Performance of 3 × 3 HRA under the lock-up faults.

| S.No. | Max output | Healthy | Fault introduced in Column-1 | | | Fault introduced in Column-1 and 2 | | | Fault introduced in Column-1, 2 and 3 | | |
|---|---|---|---|---|---|---|---|---|---|---|---|
| | | 0-fault | 1-fault (A1) | 2-faults (A1,A4) | 3-faults (A1,A4,A7) | 4-faults (A1,A4,A7,A2) | 5-faults (A1,A4,A7,A2,A5) | 6-faults (A1,A4, A7,A2,A5,A8) | 7-faults (A1,A4, A7,A2,A5,A8,A3) | 8-faults (A1 to A8) | 9-faults (A1 to A9) |
| 1 | Displacement (cm) | 7.007 | 6.002 | 5.245 | 4.661 | 3.491 | 2.789 | 2.323 | 0 | 0 | 0 |
| 2 | Force (N) | 204.4 | 182.0 | 165.4 | 151.8 | 117.7 | 95.62 | 79.96 | 970 | 485.2 | 0 |
| 3 | Velocity (cm/s) | 36.1 | 30.94 | 27.07 | 24.06 | 18.05 | 14.44 | 12.03 | 0 | 0 | 0 |

**Table 5**
Performance of 3 × 3 HRA under the short-circuit/loose faults.

| S. No. | Max output | Healthy | Fault introduced in Column-1 | | | Fault introduced in Column-1 and 2 | | | Fault introduced in Column-1, 2 and 3 | | |
|---|---|---|---|---|---|---|---|---|---|---|---|
| | | 0-fault | 1-fault (A1) | 2-faults (A1,A4) | 3-faults (A1,A4,A7) | 4-faults (A1, A4,A7,A2) | 5-faults (A1, A4,A7,A2,A5) | 6-faults (A1,A4, A7,A2,A5,A8) | 7-faults (A1,A4, A7,A2,A5,A8,A3) | 8-faults (A1 to A8) | 9-faults (A1 to A9) |
| 1 | Displacement (cm) | 7.007 | 6.227 | 5.447 | 4.668 | 3.888 | 3.109 | 2.33 | 1.6 | 0.8 | 0 |
| 2 | Force (N) | 204.4 | 179.5 | 156 | 132.6 | 109.9 | 87.14 | 64.66 | 43 | 21.6 | 0 |
| 3 | Velocity (cm/s) | 36.1 | 32.08 | 28.07 | 24.06 | 20.05 | 16.04 | 12.03 | 8.0 | 4.0 | 0 |

elements, the system remains to perform with graceful degradation. However, the tolerance to the force capability of series actuators under loose/short-circuit fault is nearly 18% less than the other types of faults.

On the other hand, The pure parallel configuration of 3 actuation elements that we studied showed an increased force capability by almost three times (i.e. from 26.8 N to 80.39 N). Although this system was able to tolerate the loose/short-circuit fault with graceful degradation of 33.4%, it failed to perform with the other two faults. The 3 × 3 HRA that was designed for this work had a combination of series and parallel elements with the capability to tolerate all types of faults. Figs. 17–19 show the performance of 3 × 3 HRA displacement, force and velocity aspects in the presence of 4 different faults tested independently. When the 3 × 3 HRA performance was studied with a single lock-up fault, the reduction of displacement was found to be a maximum of 14.34% and minimum in the presence of loose/short-circuit fault (11.13%). However, the reduction of force was recorded maximum (12.18%) in the presence of loose/short-circuit fault and minimum (10.95%) in the presence of a lock-up fault. The HRA was able to tolerate up to 6 faulty elements provided that at least one actuation element in each series is in healthy condition. The reduction in the performance of HRA depends on the number of faulty actuation elements, the type of fault and the position of the faulty actuation element in the configuration. However, the fault location in the configuration of the HRA is out of the scope of current work.

Please cite this article as: A. M. Gollapudi, V. Velagapudi and S. Korla, Modeling and simulation of a high-redundancy direct-driven linear electromechanical actuator for fault-tolerance under various fault conditions, Engineering Science and Technology, an International Journal, https://doi.org/10.1016/j.jestch.2019.12.007

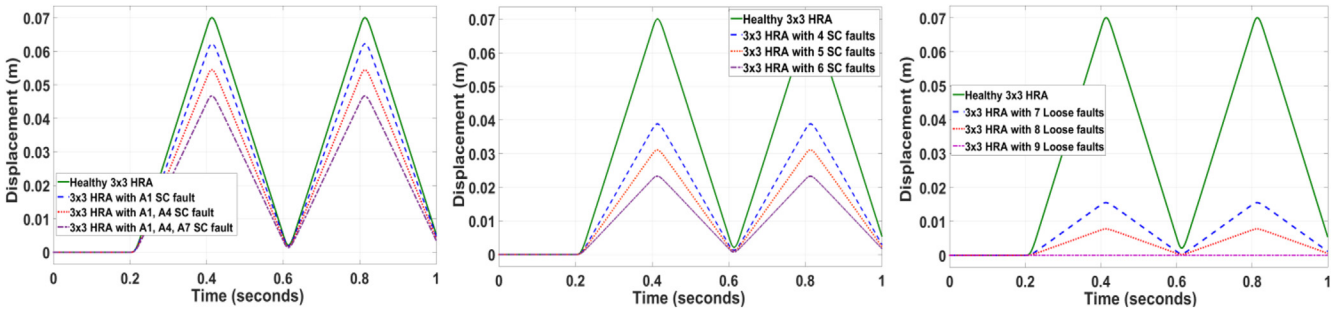


**Fig. 15a.** Displacements of 3 × 3 HRA under increasing the number of short-circuit/loose faults in the actuator from A1 to A9 (column-wise).

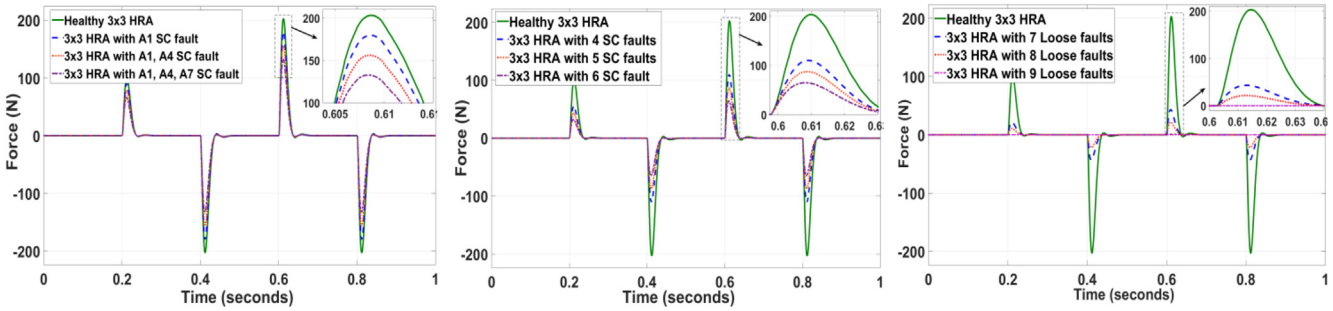


**Fig. 15b.** Forces induced due to 3 × 3 HRA under increasing the number of short-circuit/loose faults in the actuator from A1 to A9 (column-wise).

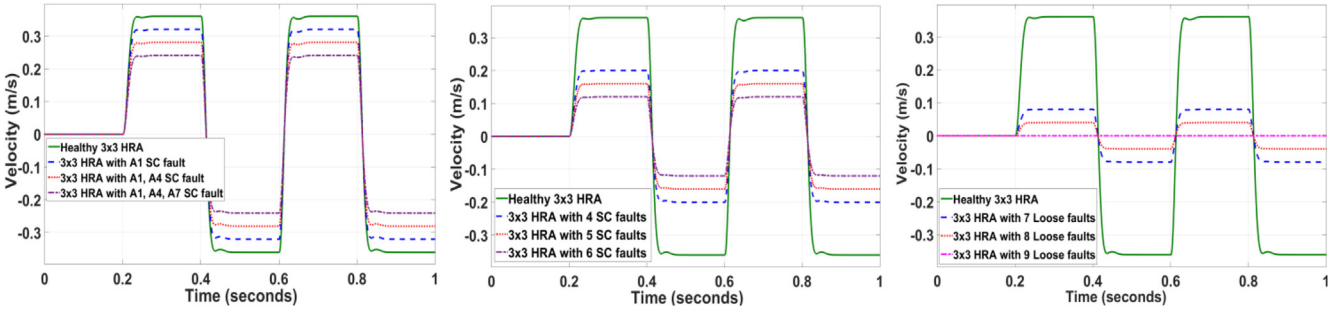


**Fig. 15c.** Velocities to 3 × 3 HRA under increasing the number of short-circuit/loose faults in the actuator from A1 to A9 (column-wise).

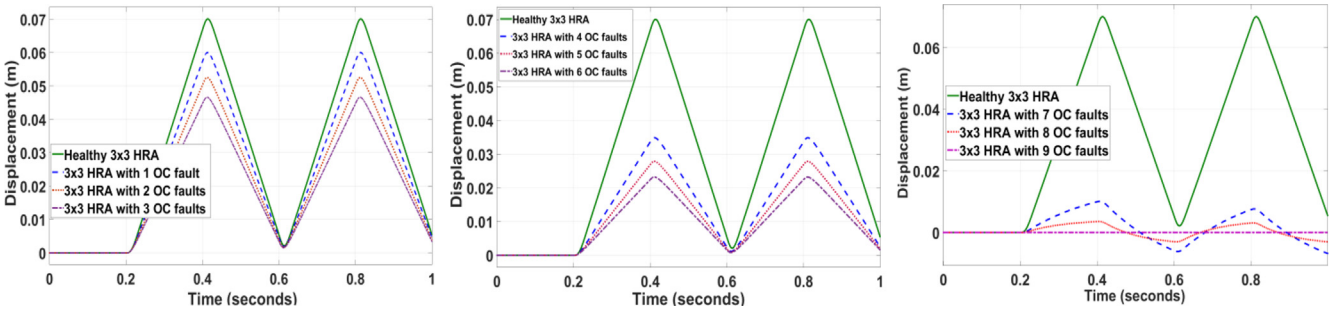


**Fig. 16a.** Displacements of 3 × 3 HRA under increasing the number of open-circuit faults in the actuator from A1 to A9 (column-wise).

Please cite this article as: A. M. Gollapudi, V. Velagapudi and S. Korla, Modeling and simulation of a high-redundancy direct-driven linear electromechanical actuator for fault-tolerance under various fault conditions, Engineering Science and Technology, an International Journal, https://doi.org/10.1016/j.jestch.2019.12.007

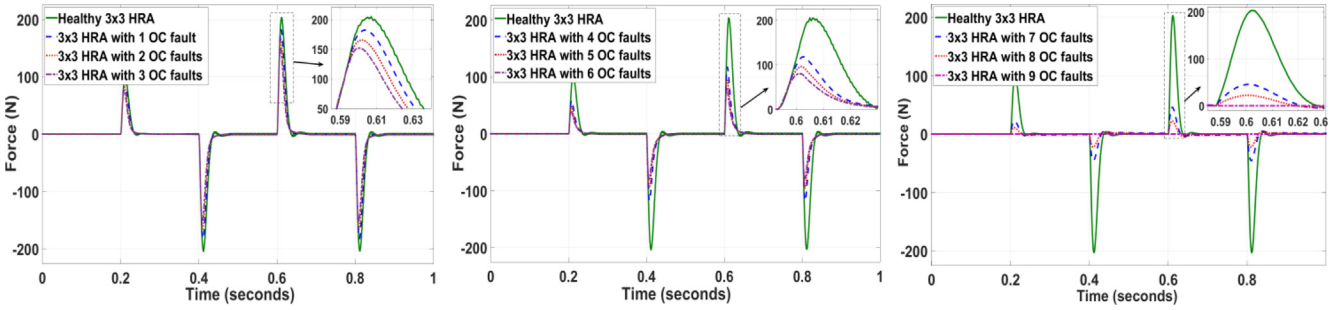


**Fig. 16b.** Forces induced due to 3 × 3 HRA under increasing the number of open-circuit faults in the actuator from A1 to A9 (column-wise).

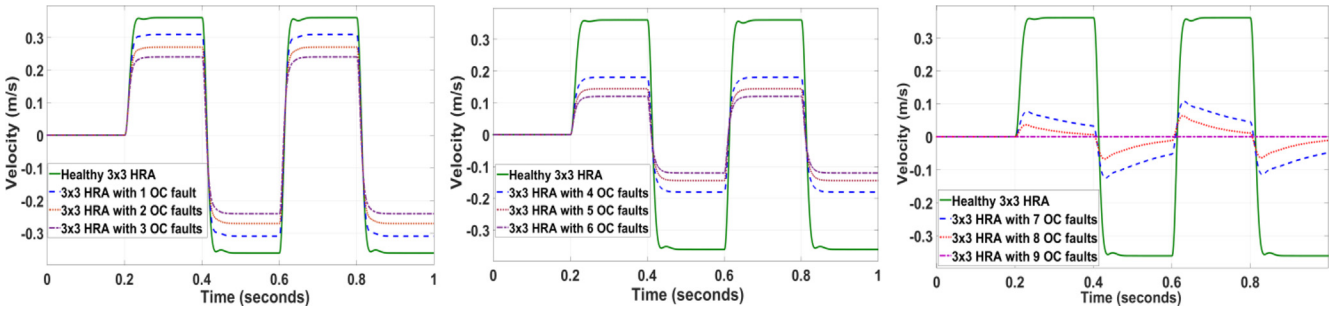


**Fig. 16c.** Velocities of 3 × 3 HRA under increasing the number of open-circuit faults in the actuator from A1 to A9 (column-wise).

**Table 6**
Performance of 3 × 3 HRA under the open-circuit faults.

| S.No. | Max output | Healthy | Fault introduced in Column-1 | | | Fault introduced in Column-1 and 2 | | | Fault introduced in Column-1, 2 and 3 | | |
|---|---|---|---|---|---|---|---|---|---|---|---|
| | | 0-fault | 1-fault (A1) | 2-faults (A1,A4) | 3-faults (A1, A4,A7) | 4-faults (A1, A4,A7,A2) | 5-faults (A1,A4, A7,A2,A5) | 6-faults (A1,A4,A7, A2,A5,A8) | 7-faults (A1,A4,A7, A2,A5,A8,A3) | 8-faults (A1 to A8) | 9-faults (A1 to A9) |
| 1 | Displacement (cm) | 7.007 | 6.03 | 5.3 | 4.7 | 3.6 | 2.9 | 2.3 | 1.0 | 0.4 | 0 |
| 2 | Force (N) | 204.4 | 181 | 159 | 137.2 | 113.6 | 90.2 | 67.2 | 45.7 | 22.4 | 0 |
| 3 | Velocity (cm/s) | 36.1 | 31.0 | 27.0 | 24.0 | 18.0 | 15.0 | 12.0 | 5.0 | 2.0 | 0 |

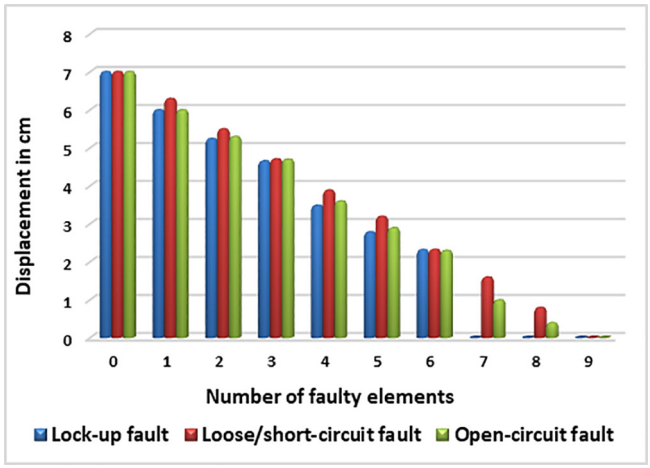


**Fig. 17.** Comparison of displacements of a 3 × 3 HRA under the lock-up, open-circuit and short-circuit/loose faults.

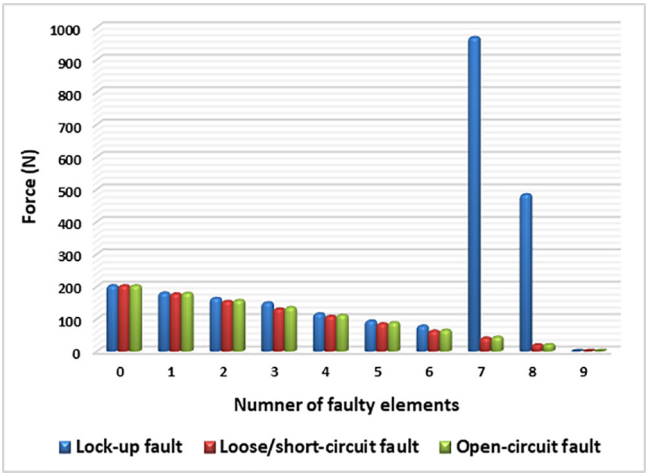


**Fig. 18.** Comparison of forces of a 3 × 3 HRA under the lock-up, open-circuit and short-circuit/loose faults.

Please cite this article as: A. M. Gollapudi, V. Velagapudi and S. Korla, Modeling and simulation of a high-redundancy direct-driven linear electromechanical actuator for fault-tolerance under various fault conditions, Engineering Science and Technology, an International Journal, https://doi.org/10.1016/j.jestch.2019.12.007

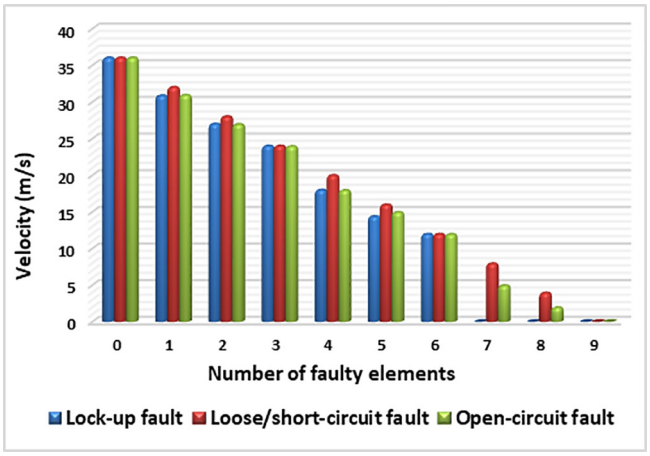


**Fig. 19.** Comparison of velocities of a 3 × 3 HRA under the lock-up, open-circuit and short-circuit/loose faults.

## Declaration of Competing Interest

The authors declare that they have no known competing financial interests or personal relationships that could have appeared to influence the work reported in this paper.

## Acknowledgments

The authors are thankful to Media Lab Asia, The Department of Electronics and Information Technology (DEITY), India, for sponsoring this research work under the Visvesvaraya Ph.D scheme of DEITY, 2014.

## References

[1] X. Du, R. Dixon, LQG control of a high redundancy actuator, Mechatr. IEEE 44 (2007) (2007) 1–6, https://doi.org/10.1109/AIM.2007.4412598.

[2] G.A. Manohar, V. Vasu, K. Srikanth, Modeling and simulation of high redundancy actuator for fault-tolerance, Mater. Today Proc. 5 (2018) 18867–18873, https://doi.org/10.1016/j.matpr.2018.06.234.

[3] S.D. Bemment, R.M. Goodall, R. Dixon, C.P. Ward, Improving the reliability and availability of railway track switching by analysing historical failure data and introducing functionally redundant subsystems, Proc. Inst. Mech. Eng. Part F J. Rail Rapid Transit. (2017) 1–18, https://doi.org/10.1177/0954409717727879.

[4] G. Qiao, G. Liu, Z. Shi, Y. Wang, S. Ma, T.C. Lim, A review of electromechanical actuators for more/all electric aircraft systems, Proc. Inst. Mech. Eng., Part C 232 (22) (2018) 4128–4151, https://doi.org/10.1177/0954406217749869.

[5] S. Kwon, J. Cheon, J. Lee, C. Kim, S. Kim, A. Design, Implementation of a fault-tolerant rod control system for nuclear power plants, Ind. Electron. IEEE Int. Symp. 3 (2006) (2006) 1933–1936, https://doi.org/10.1109/isie.2006.295868.

[6] J. Davies, T. Steffen, R. Dixon, R.M. Goodall, A. Zolotas, J. Pearson, Modelling of high redundancy actuation utilising multiple moving coil actuators, IFAC (2008), https://doi.org/10.3182/20080706-5-KR-1001.0482.

[7] H. Antong, R. Dixon, C. Ward, Modelling and building of experimental rig for high redundancy actuator, Int. Conf. Control. 2014 (2014) 384–388, https://doi.org/10.1109/CONTROL.2014.6915171.

[8] X. Du, R. Dixon, R.M. Goodall, A.C. Zolotas, Mechatronics modelling and control of a high redundancy actuator, Mechatronics 20 (2010) 102–112, https://doi.org/10.1016/j.mechatronics.2009.09.009.

[9] R. Dixon, T. Steffen, J. Davies, R.M. Goodall, A.C. Zolotas, J. Pearson, X. Du, HRA – intrinsically fault tolerant actuation through high redundancy, IFAC Proc. (2009) 1216–1221, https://doi.org/10.3182/20090630-4-ES-2003.0099.

[10] J. Davies, H. Tsunashima, R.M. Goodall, R. Dixon, T. Steffen, Fault detection in High Redundancy Actuation using an interacting multiple-model approach, IFAC Proc. (2009) 1228–1233, https://doi.org/10.3182/20090630-4-ES-2003.0094.

[11] J. Davies, T. Steffen, R. Dixon, R. Goodall, A. Zolotas, Active versus passive fault tolerant control of a High Redundancy Actuator, Eur. Control Conf. (2009) 3671–3676, https://doi.org/10.23919/ECC.2009.7074970.

[12] H. Antong, R. Dixon, C.P. Ward, High redundancy actuator with 12 elements: open- and closed-loop model validation, IFAC-Papers Online 49 (2016) 254–259, https://doi.org/10.1016/j.ifacol.2016.10.563.

[13] M.S. Kim, S.C. Chung, A systematic approach to design high-performance feed drive systems, Int. J. Mach. Tools Manuf. 45 (2005) 1421–1435, https://doi.org/10.1016/j.ijmachtools.2005.01.032.

[14] R.J. Patton, Fault detection and diagnosis in aerospace systems using analytical redundancy, Comput. Control Eng. 8 (1991) 127–136, https://doi.org/10.1049/cce:19910031.

[15] A.J. Chirico, J.R. Kolodziej, A data-driven methodology for fault detection in electromechanical actuators, J. Dyn. Syst. Meas. Control. Trans. ASME 136 (2014) 1–16, https://doi.org/10.1115/1.4026835.

Please cite this article as: A. M. Gollapudi, V. Velagapudi and S. Korla, Modeling and simulation of a high-redundancy direct-driven linear electromechanical actuator for fault-tolerance under various fault conditions, Engineering Science and Technology, an International Journal, https://doi.org/10.1016/j.jestch.2019.12.007